

Performance Investigation of Electrochemical Assisted $\text{HClO}/\text{Fe}^{2+}$ Process For The Treatment of Landfill Leachate

Zhihong Ye

Chongqing University

Fei Miao

Wuhan University

Hui Zhang (✉ eeeng@whu.edu.cn)



Wuhan University <https://orcid.org/0000-0002-2508-4912>

Research Article

Keywords: Advanced oxidation process, Active chlorine, Electrochemical Fenton-type process, Landfill leachate, COD, NH_4^+-N

Posted Date: November 12th, 2021

DOI: <https://doi.org/10.21203/rs.3.rs-888579/v1>

License:   This work is licensed under a Creative Commons Attribution 4.0 International License.
[Read Full License](#)

Version of Record: A version of this preprint was published at Environmental Science and Pollution Research on February 16th, 2022. See the published version at <https://doi.org/10.1007/s11356-022-19174-2>.

**Performance investigation of electrochemical assisted
HClO/Fe²⁺ process for the treatment of landfill leachate**

Zhihong Ye ^{1,2}, Fei Miao¹, Hui Zhang^{1,*}

¹ *Department of Environmental Science and Engineering, School of Resource and Environmental
Sciences, Wuhan University, Wuhan 430079, China*

² *Key Laboratory of Eco-environments in Three Gorges Reservoir Region, Ministry of Education,
College of Environment and Ecology, Chongqing University, Chongqing, China*

Paper submitted for publication in *Environmental Science and Pollution Research*

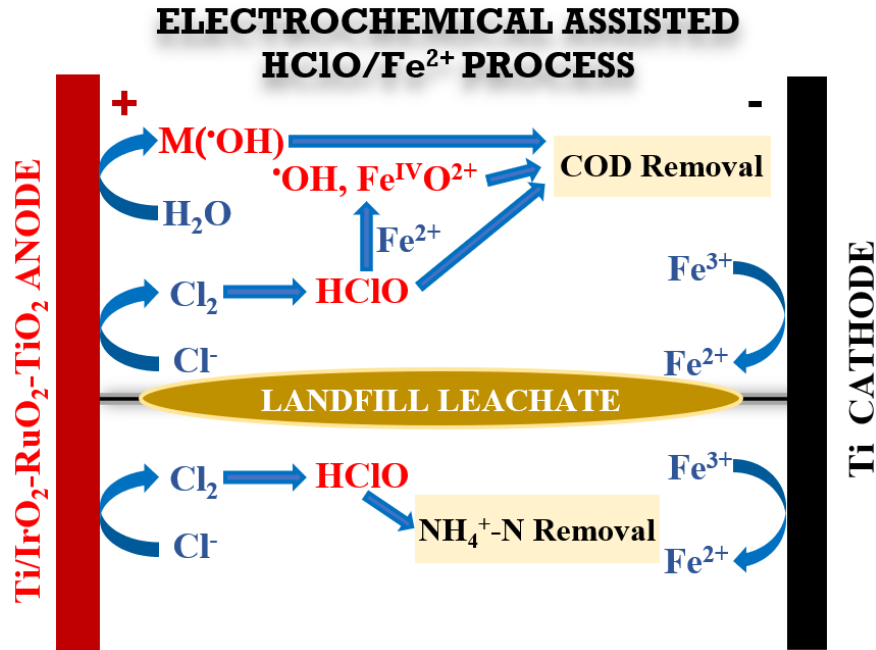
* Corresponding author: eeng@whu.edu.cn

Abstract

The feasibility of removal of COD and ammonia nitrogen ($\text{NH}_4^+\text{-N}$) from landfill leachate by electrochemical assisted $\text{HClO}/\text{Fe}^{2+}$ process is demonstrated for the first time. The performance of active chlorine generation at the anode was evaluated in $\text{Na}_2\text{SO}_4/\text{NaCl}$ media, and a higher amount of active chlorine was produced at greater chloride concentration and higher current density. The probe experiments confirmed the coexistence of hydroxyl radical ($\bullet\text{OH}$) and Fe(IV)-oxo complex ($\text{Fe}^{\text{IV}}\text{O}^{2+}$) in the $\text{HClO}/\text{Fe}^{2+}$ system. The influence of initial pH, Fe^{2+} concentration and applied current density on COD and $\text{NH}_4^+\text{-N}$ abatement was elaborately investigated. The optimum pH was found to be 3.0, and the proper increase in Fe^{2+} dosage and current density resulted in higher COD removal due to the accelerated accumulation of $\bullet\text{OH}$ and $\text{Fe}^{\text{IV}}\text{O}^{2+}$ in the bulk liquid phase. Whereas, the $\text{NH}_4^+\text{-N}$ oxidation was significantly affected by the applied current density because of the effective active chlorine generation at high current, but was nearly independent of Fe^{2+} concentration. The reaction mechanism of electrochemical assisted $\text{HClO}/\text{Fe}^{2+}$ treatment of landfill leachate was finally proposed. The powerful $\bullet\text{OH}$ and $\text{Fe}^{\text{IV}}\text{O}^{2+}$, in concomitance with active chlorine and $\text{M}(\bullet\text{OH})$ were responsible for COD abatement and active chlorine played a key role in $\text{NH}_4^+\text{-N}$ oxidation. The proposed electrochemical assisted $\text{HClO}/\text{Fe}^{2+}$ process is a promising alternative for the treatment of refractory landfill leachate.

Keywords: Advanced oxidation process; Active chlorine; Electrochemical Fenton-type process; Landfill leachate; COD; $\text{NH}_4^+\text{-N}$

Graphical abstract



Introduction

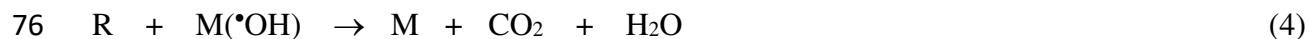
Sanitary landfill disposal is the most widely used method for municipal solid waste treatment in the world due to its economic advantages (Wu et al. 2018). However, this disposal method leads to the production of complex liquids, namely landfill leachate, containing large amounts of organic pollutants, $\text{NH}_4^+\text{-N}$, inorganic salts and heavy metals (Fu et al. 2021). The generation of landfill leachate is expected to approach 330 million tonnes by 2025, posing great challenges to water environment and ecosystem worldwide (Abunama et al. 2018; Costa et al. 2019). The characteristics of leachate are affected by various factors including waste origin, seasonal precipitation and, particularly, the age of landfill (Panizza et al. 2010). The old landfill leachate (more than 10 years) usually has stable water quality indexes, such as high fraction of recalcitrant organics, high $\text{NH}_4^+\text{-N}$ concentration (2000-5000 mg L^{-1}) and low BOD/COD ratio (< 0.1),

making it difficult to be treated using traditional biological technology (Deng et al. 2021; Ghahrchi and Rezaee 2021). Many alternative physical and chemical methods have been applied for the treatment of landfill leachate, such as flocculation and sedimentation (Silva et al. 2004), adsorption (Reshadi et al. 2020), ozonation (Yang et al. 2021), advanced oxidation processes (Kwarciak-Kozłowska and Fijałkowski 2021), membrane treatment (Keyikoglu et al. 2021) and electrochemical technologies (Deng et al. 2020).

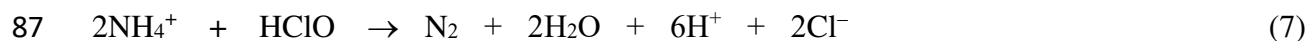
Among them, electrochemical methods are considered to be the most promising technologies that can effectively destroy refractory organics and increase the biodegradability of the leachate for the subsequent biological treatment (El Kateb et al. 2019). And electro-oxidation (EO), one of the electrochemical advanced oxidation processes (EAOPs), shows great priority for industrialization because of its stability, easy operation and amenability to automation (Fernandes et al. 2015). During EO, the powerful physisorbed hydroxyl radical ($M(\bullet OH)$) is generated via water oxidation on the surface of anode M (reaction 1), and it can be transformed into the chemisorbed active oxygen or superoxide MO from reaction (2), especially for active anodes like IrO_2 and RuO_2 (Moreira et al. 2017).



The presence of these active species allows efficient refractory organics (R) removal in landfill leachate by the approaches of (i) electrochemical conversion, that arises from MO/M pair mediator via reaction (3) and (ii) electrochemical combustion, that is caused by the weakly interacted $M(\bullet OH)$ via reaction (4) (Sirés and Brillas 2012; Sirés et al. 2014).

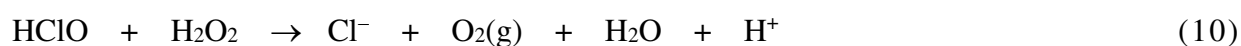
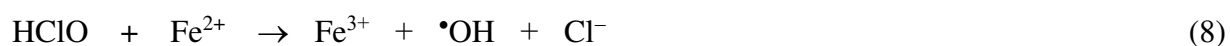


77 Unfortunately, the above active species play negligible roles in NH_4^+ -N oxidation during the
 78 treatment of landfill leachate (Bunce and Bejan 2011). The high concentration of Cl^- in the
 79 leachate can compete with water to be oxidized to dissolved chlorine via reaction (5), which is
 80 further converted into hypochlorous acid ($HClO$, $E^0 = 1.49 \text{ V/SHE}$) at pH 3.0-8.0 through
 81 reaction (6). This gives rise to the so-called EO- $HClO$ process (Murrieta et al. 2020; Sirés et al.
 82 2014). The electro-generated active chlorine thus becomes the dominant oxidant for NH_4^+ -N
 83 degradation according to the stoichiometry reaction (7), and also acts as a strong oxidizer to
 84 destroy some organic pollutants (Cabeza et al. 2007).



88 Recently, Kishimoto et al. (2015) proposed a new electrochemical assisted Fenton-like process
 89 to form $\bullet OH$ using Fe^{2+} and $HClO$ via reaction (8) for the decontamination of wastewater
 90 containing Cl^- , while Fe^{2+} can be regenerated upon cathodic reduction of Fe^{3+} through reaction
 91 (9). This electro-Fenton-like process shows numerous advantages over the conventional electro-
 92 Fenton. Firstly, $HClO$ is generated by the chlorine-based reaction (5) and (6) at the anode,
 93 avoiding the competing cathodic reduction of O_2 to H_2O_2 and Fe^{3+} to Fe^{2+} occurred in the electro-
 94 Fenton system. Secondly, 2 mol of electrons can be used to generate 1 mol of $\bullet OH$
 95 stoichiometrically, whereas the conventional electro-Fenton requires 3 mol for 1 mol of $\bullet OH$.

Finally, during the electro-Fenton treatment of wastewater with high Cl^- content, the electro-generated HClO would consume H_2O_2 via the adverse reaction (10), resulting in a huge waste of oxidants (Aguilar et al. 2017; Murrieta et al. 2020; Shah et al. 2015). This can be overcome in the electro-Fenton-like process in which HClO is electro-generated and H_2O_2 could not be produced. Moreover, a recent work suggested that the high valent iron complex, $\text{Fe}^{\text{IV}}\text{O}^{2+}$ ($[\text{Fe}^{\text{IV}}=\text{O}]^{2+}$, $E^0 = 2.0 \text{ V/SHE}$), should be an important reactive species produced from the reaction between HClO and Fe^{2+} (reaction 11), which was neglected by the previous studies (Liang et al. 2020).



The objective of this study was to investigate, for the first time, the performance of electrochemical assisted $\text{HClO}/\text{Fe}^{2+}$ process regarding the treatment of old landfill leachate. The ability to generate HClO of the anode was firstly evaluated by conducting the electrolysis in NaCl or mixed $\text{Na}_2\text{SO}_4 + \text{NaCl}$ media at pH 3.0 with different chloride concentrations and current densities in the absence of Fe^{2+} . The formation of $\bullet\text{OH}$ and $\text{Fe}^{\text{IV}}\text{O}^{2+}$ in the $\text{HClO}/\text{Fe}^{2+}$ system was further confirmed by using dimethyl sulfoxide (DMSO) and methyl phenyl sulfoxide (PMSO) as the radical probes, respectively (Shao et al. 2018). Then, the effect of initial pH, Fe^{2+} concentration and current density on COD and $\text{NH}_4^+\text{-N}$ decay was examined during the

electrochemical assisted $\text{HClO}/\text{Fe}^{2+}$ treatment of landfill leachate. At last, a specific reaction mechanism for COD and $\text{NH}_4^+\text{-N}$ removal was proposed.

Experimental

Landfill leachate characteristics

The old landfill leachate was collected from a municipal sanitary landfill located in Wuhan, China. The samples were stored in a refrigerator at 4 °C to maintain the characteristics unaltered, and they were directly used in electrochemical systems without any pre-treatment (Ye et al. 2016). The main characteristics of the leachate were summarized in Table 1.

Identification of $\bullet\text{OH}$ and $\text{Fe}^{\text{IV}}\text{O}^{2+}$

DMSO was selected as a molecular probe for the detection of $\bullet\text{OH}$ in the $\text{HClO}/\text{Fe}^{2+}$ system. It can react rapidly with $\bullet\text{OH}$ leading to the formation of methanesulfonic acid and methyl radicals, followed by several reactions to generate the final product formaldehyde (HCHO) (Tai et al. 2004; Zhang et al. 2020). Thus, the quantitative analysis of $\bullet\text{OH}$ in this study was conducted through the determination of the concentration of HCHO in the solution. In addition, it is generally believed that $\text{Fe}^{\text{IV}}\text{O}^{2+}$ can oxidize PMSO through oxygen transfer to generate methyl phenyl sulfone (PMSO_2), which is different from the $\bullet\text{OH}$ induced hydroxylated products (Fang et al. 2022). To figure out whether $\text{Fe}^{\text{IV}}\text{O}^{2+}$ was generated in $\text{HClO}/\text{Fe}^{2+}$ system, PMSO was selected as the chemical probe to distinguish $\text{Fe}^{\text{IV}}\text{O}^{2+}$ from $\bullet\text{OH}$. The detailed procedures for the identification of $\bullet\text{OH}$ and $\text{Fe}^{\text{IV}}\text{O}^{2+}$ in the $\text{HClO}/\text{Fe}^{2+}$ system were described in Supplementary Material (Text S1).

Electrochemical systems

A single-cell rectangular electrolytic reactor was used in the experiments and the size of which was 12 cm×10 cm×20 cm. The anodic material was titanium coated by iridium dioxide, ruthenium dioxide and titanium dioxide (Ti/IrO₂-RuO₂-TiO₂, 75 cm²) and the cathodic material was titanium. The gap between the anode and the cathode was adjusted parallel at a distance of 2 cm. All trials were conducted under constant current conditions provided by a direct current (DC) power supply (LW-3030KD) under room temperature at 20 ± 3 C, and the solution was vigorously stirred with a magnetic bar at 700 rpm. The assessment of the ability to generate HClO at the anode was firstly carried out with 400 mL NaCl or mixed Na₂SO₄ + NaCl solutions at pH 3.0 in the absence or presence of Fe²⁺ under the conditions of different chloride concentration and current density. The trials for the treatment of landfill leachate were performed under galvanostatic conditions with the volume of 1000 mL and the electrodes working area of 75 cm². Samples were collected to analyze the COD and NH₄⁺-N concentrations at pre-selected time interval.

Analytical procedures

The solution pH was measured with a Mettler-Toledo FE20 pH meter. Active chlorine was determined by the N, N-diethyl-p-phenylenediamine (DPD) colorimetric method using a UV/vis spectrophotometer (UV-5000, METASH) set at $\lambda = 515$ nm (Murrieta et al. 2020). The concentration of Fe²⁺ was analyzed by measuring the absorption of the reddish solutions resulting upon its complexation with 1,10-phenantroline, whose maximum absorbance was at $\lambda = 510$ nm (Ye et al. 2020). COD was determined by a fast digestion-spectrophotometric method based on

the Standard of the People's Republic of China for Environmental Protection (Ye et al. 2016). $\text{NH}_4^+\text{-N}$ concentration was measured using Nessler's reagent colorimetric method. The concentration of HCHO was analyzed using acetylacetone method with a UV/vis spectrophotometer set at $\lambda = 412 \text{ nm}$ (Zhang et al. 2020). PMSO and PMSO₂ were analyzed using a high-performance liquid chromatograph (HPLC, Shimadzu Co.) with a LC-20AB pump and a SPD-20A chromatograph equipped with a C-18 column ($250 \times 4.6 \text{ mm}$, $5 \mu\text{m}$) and an SPD-10A UV-visible detector. The elution was achieved upon recirculation of an 80:20 (v:v) water/acetonitrile mixture at 1.0 mL min^{-1} . The detection wavelengths for PMSO and PMSO₂ were set at 230 and 215 nm, respectively (Lai et al. 2020).

Results and discussion

Active chlorine production on Ti/IrO₂-RuO₂-TiO₂ anode

To clarify the ability of Ti/IrO₂-RuO₂-TiO₂ anode for the production of active chlorine, the variation of active chlorine content as function of electrolysis time in EO-HClO process was monitored at various levels of chloride ions concentration and different current densities. As depicted in Fig. 1(a), the accumulated active chlorine content rapidly increased with the increase of Cl^- concentration from 1.0 to 3.0 g L^{-1} , and further increase the Cl^- concentration to 4.0 g L^{-1} led to the maximal active chlorine production (967 mg L^{-1}), despite the enhancement was insignificant. The surface catalytic properties of anodes toward chloride ion oxidation have substantial relevance to the generation of active chlorine. The low adsorption properties of the active IrO₂-RuO₂-TiO₂ anode benefit the active chlorine production since a large number of

empty active sites are available for Cl^- oxidation (Garcia-Espinoza et al. 2018). Thus, the increase in Cl^- concentration can accelerate the accessibility between Cl^- and active sites on the anode surface, and promote active chlorine production.

The effect of current density on active chlorine generation was further investigated at 4.0 g L^{-1} of Cl^- ion. As shown in Fig. 1(b), a larger accumulation of active chlorine was achieved as the current density became higher. Only 550 mg L^{-1} active chlorine was yielded at the lowest current density 7.5 mA cm^{-2} , which was dramatically enhanced up to 967 and 1397 mg L^{-1} at 15 and 20 mA cm^{-2} , respectively. The active chlorine concentration reached a maximum 1670 mg L^{-1} after 180 min electrolysis at 30 mA cm^{-2} . Obviously, the increase in current density could enhance charge transfer in the electrochemical process, thus, facilitating the Cl^- oxidation on the anode. However, the applied current was partly invested in the parallel parasitic reactions such as water oxidation at higher current density, resulting in the decreased current efficiency of active chlorine generation (Murrieta et al. 2020).

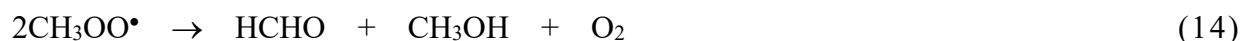
In order to better understand the electrochemical assisted $\text{HClO}/\text{Fe}^{2+}$ process, the evolution of active chlorine and Fe^{2+} concentrations was investigated in the presence of 4.0 g L^{-1} of Cl^- ion and 5.6 mM of Fe^{2+} ion at current density of 15 mA cm^{-2} . Fig. 2(a) highlights the much slower accumulation of active chlorine in the electrochemical assisted $\text{HClO}/\text{Fe}^{2+}$ system, which confirmed the continuous consumption of active chlorine by the Fenton-like reaction (8) and nonradical reaction (11). Worth noting, the accumulated active chlorine was lower than 40 mg L^{-1} during the initial 30 min reaction, whereas its counterpart reached up to 430 mg L^{-1} in the EO-HClO system without Fe^{2+} , indicating the rapid consumption of active chlorine at the initial

stage. This is consistent with the result achieved on Fe^{2+} evolution in Fig. 2(b), Fe^{2+} concentration underwent a very quick decay once the reaction initiated, and reached 96% disappearance at 30 min. Therefore, it is believed that the ability of the cathode to reduce Fe^{3+} by reaction (9) became the rate limited factor after 30 min of electrochemical assisted $\text{HClO}/\text{Fe}^{2+}$ process, rather than active chlorine concentration.

Identification of reactive species involved in the $\text{HClO}/\text{Fe}^{2+}$ process

It has been reported that $\bullet\text{OH}$ is believed to be the predominant reactive species generated in the $\text{HClO}/\text{Fe}^{2+}$ process via Fenton-like reaction (8) (Aguilar et al. 2017; Kishimoto et al. 2015). However, most recently, some researchers suggested that $\text{Fe}^{\text{IV}}\text{O}^{2+}$ could also make a significant contribution to wastewater decontamination (Liang et al. 2020). Therefore, to fully identify the potential reactive species involved in the $\text{HClO}/\text{Fe}^{2+}$ process, DMSO was used as a capturing agent for $\bullet\text{OH}$, and PMSO was selected to determine $\text{Fe}^{\text{IV}}\text{O}^{2+}$ by measuring the conversion rate of PMSO to PMSO_2 in this work.

DMSO has been widely employed in the detection of $\bullet\text{OH}$ in advanced oxidation processes due to its high reactivity with $\bullet\text{OH}$ ($k = 4.5\sim 7.1 \times 10^9 \text{ M}^{-1}\text{s}^{-1}$) forming methanesulfinic acid and methyl radicals via reaction (12), the generated methyl radicals were further converted to HCHO thorough reaction (13) and (14) (Tai et al. 2004). Thus, the presence of HCHO could provide convictive evidence for the formation of $\bullet\text{OH}$.



As shown in Fig. 3, 200 μM HCHO was finally detected in the $\text{HClO}/\text{Fe}^{2+}$ system in the presence of excess DMSO after 30 min reaction at pH 3.0, indicating the formation of $\bullet\text{OH}$ via Fenton-like reaction (8).

Moreover, identification of $\text{Fe}^{\text{IV}}\text{O}^{2+}$ was performed using PMSO as the probe according to reaction (15), the formation of $\text{Fe}^{\text{IV}}\text{O}^{2+}$ species could be assessed on the basis of the yield of PMSO_2 (mole of PMSO_2 formed per mole of PMSO consumed, $\eta[\text{PMSO}_2] = ([\text{PMSO}_2]_{\text{formed}}/[\text{PMSO}]_{\text{consumed}} \times 100\%)$, and high production of $\text{Fe}^{\text{IV}}\text{O}^{2+}$ was suggested when $\eta[\text{PMSO}_2]$ approached 100% (Gao et al. 2020).



As depicted in Fig. 3, the $\eta[\text{PMSO}_2]$ value was quantified to be as high as 100%, suggesting the significant role of high-valent iron species in the $\text{HClO}/\text{Fe}^{2+}$ system. Note that, although $\text{Fe}(\text{IV})$ is less reactive than $\bullet\text{OH}$, it is more inert to the interference of coexisting anions (Cl^- , NO_3^- and CO_3^{2-}) and can selectively oxidize target refractory organic contaminants in wastewater (Zong et al. 2021). This finding is consistent with the previous work documenting $\text{Fe}^{\text{IV}}\text{O}^{2+}$ as the main oxidant in $\text{HClO}/\text{Fe}^{2+}$ system (Liang et al. 2020). Summarily, the coexistence of HClO -simulated one-electron pathway to $\bullet\text{OH}$ and two-electron nonradical transformation of Fe^{2+} to $\text{Fe}^{\text{IV}}\text{O}^{2+}$ is identified, and these two reactive species may together contribute to the degradation of organic pollutants during wastewater treatment.

Electrochemical assisted $\text{HClO}/\text{Fe}^{2+}$ treatment of landfill leachate

The old landfill leachate was firstly treated by EO- HClO in the absence of Fe^{2+} at different current density (7 and 14 mA cm^{-2} , respectively). As shown in Fig. S1, only 8.1% COD

abatement was obtained after 2 h treatment at low current density 7 mA cm^{-2} , and further increase in the current density to 14 mA cm^{-2} led to slight enhancement on COD removal (13.7%). The old landfill leachate is usually characterized by complex refractory organic compounds, such as humic and fulvic acids, which are highly resistant to the oxidation. The active anode, $\text{Ti/IrO}_2\text{-RuO}_2\text{-TiO}_2$, used in this study presents low oxygen evolution potential and allows the generation of a small amount of unstable $\text{M}(\bullet\text{OH})$, which is too weak to yield efficient oxidation of organic pollutants (Sirés et al. 2014). On the other hand, despite the excellent ability to form active chlorine from the oxidation of chloride at the anode, as displayed in Fig. 1, the oxidative power of HOCl ($E^0=1.49\text{V}$ vs. SHE) is barely satisfactory to acquire quick COD abatement due to the accumulation of persistent chloroderivatives (Panizza et al. 2010).

Similar results were achieved for $\text{NH}_4^+\text{-N}$ treatment in EO-HClO system, i.e., 7.3% and 9.1% removal efficiency at current density of 7 and 14 mA cm^{-2} , respectively. As reported, the contribution of $\bullet\text{OH}$ on $\text{NH}_4^+\text{-N}$ oxidation is assumed as negligible, active chlorine thus became the dominant active species for the elimination of $\text{NH}_4^+\text{-N}$, which was also competitively consumed by high amounts of organics in landfill leachate (Mandal et al. 2020). Summarily, single EO-HClO process failed to achieve powerful performance on landfill leachate treatment.

Effect of initial pH

To investigate the effect of initial pH on COD and $\text{NH}_4^+\text{-N}$ removal, experiments were carried out with a current density of 14 mA cm^{-2} and Fe^{2+} dosage of 4.0 mM at different initial pH (2.0, 3.0 and 9.0). The decay of COD and $\text{NH}_4^+\text{-N}$ as a function of time is displayed in Fig. 4. Similar COD removal efficiencies, 55.2% and 55.8%, were achieved after 8 h treatment at initial pH 2.0

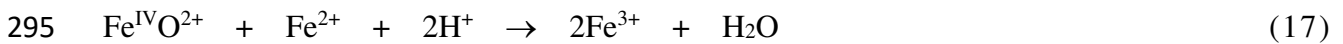
and 3.0, whereas the value was dropped to 28% when the pH increased to 9.0. Worth noting, the initial 30 min treatment already led to 45% COD abatement at pH 3.0, which was much higher than that obtained in EO-HClO process (3%), and the following 7.5 h treatment only contributed 10.8% more COD removal. This highly agrees with the results achieved in Section 3.1, where it has been demonstrated that the production of $\bullet\text{OH}$ and $\text{Fe}^{\text{IV}}\text{O}^{2+}$ from reactions (8) and (11) largely occurred during the initial stage due to the presence of high concentration of Fe^{2+} . In consequence, the COD abatement in electrochemical assisted $\text{HClO}/\text{Fe}^{2+}$ process occurred in two consecutive stages (i) the first one, where the $\bullet\text{OH}$ and $\text{Fe}^{\text{IV}}\text{O}^{2+}$ had the leading role, followed by (ii) a second one, where COD was mainly destroyed by $\text{M}(\bullet\text{OH})$ and HClO , coupled with poor contribution of $\bullet\text{OH}$ and $\text{Fe}^{\text{IV}}\text{O}^{2+}$ that generated due to the gradual reduction of Fe^{3+} at the cathode. Further increase the pH to 9.0 resulted in massive precipitation of iron species and transformation of HClO to weaker oxidant hypochlorite ion (ClO^- , pK_a for HClO/ClO^- was 7.5), these clearly explained the poor performance on COD decay at initial pH 9.0 (Ye et al. 2016).

Fig. 4 also illustrates approximately 25% $\text{NH}_4^+\text{-N}$ removal at initial pH 2.0 and 3.0, slightly higher than that achieved at pH 9.0. However, several previous studies stated that initial pH exerted little impact on $\text{NH}_4^+\text{-N}$ degradation due to the fact that $\text{NH}_4^+\text{-N}$ removal mainly takes place close to the anode surface where the local pH is minimally affected by initial pH (Vanlangendonck et al. 2005; Zhang et al. 2018). The different results obtained in this study could be attributed to the formation of complex between ammonia and Fe^{IV} species, as reported in the literature, which reduced the amount of detectable $\text{NH}_4^+\text{-N}$ in the solution (Feng et al. 2017). The generation of Fe^{IV} was significantly hampered due to the massive precipitation of ion

species at alkaline pH.

Effect of Fe²⁺ concentration

The influence of Fe²⁺ concentration, ranging from 2.0 mM to 8.0 mM, on the performance of electrochemical assisted HClO/Fe²⁺ treatment of landfill leachate was examined at initial pH 3.0 and current density 14 mA cm⁻². As can be observed in Fig. 5, the COD removal efficiency increased from 48.5% to 55.8% when Fe²⁺ dosage increased from 2.0 to 4.0 mM, but further increase in Fe²⁺ concentration to 8.0 mM led to negligible promotion in COD decay. The enhancement of HClO decomposition to active •OH and Fe^{IV}O²⁺ species can be achieved by appropriate increase in Fe²⁺ concentration, but excess Fe²⁺ also gave rise to the competitive consumption of •OH and Fe^{IV}O²⁺ via reaction (16) and (17), especially at the initial stage when HClO accumulation was insufficient, negatively affecting the COD destruction (Murrieta et al. 2020; Wang et al. 2018).



In addition, the aforementioned rate limited factor after the disappearance of added Fe²⁺ is the Fe³⁺ reduction ability of the cathode, rather than the total concentration of iron species. The generated excess Fe³⁺ from reaction (8) and (11) tended to precipitate on the cathode surface due to the formation of OH⁻ by water splitting reaction, which retarded the regeneration of Fe²⁺ via reaction (9).

The profiles of NH₄⁺-N removal with different Fe²⁺ dosage possessed similar trends during 8 h treatment, as depicted in Fig. 5. This is because NH₄⁺-N elimination is mainly attributed to the

indirect oxidation by active chlorine generated via chloride oxidation at the anode, rather than $\bullet\text{OH}$ and $\text{Fe}^{\text{IV}}\text{O}^{2+}$ species, whose production highly relied on Fe^{2+} concentration.

Effect of current density

Fig. 6 displayed the trends of the COD and $\text{NH}_4^+\text{-N}$ with electrolysis time during the treatment of landfill leachate at different current densities (7.0, 14 and 28 mA cm^{-2}) with 4.0 mM Fe^{2+} at initial pH 3.0. The COD decay was accelerated at higher current density, achieving 43.7% and 51.8% removal efficiencies at 7.0 and 14 mA cm^{-2} , respectively. This enhancement could be attributed to the increase in rate of reaction (1), (5) and (9), which led to the formation of larger amounts of $\text{M}(\bullet\text{OH})$, active chlorine and faster regeneration of Fe^{2+} , and consequently promoted the production of active $\bullet\text{OH}$ and $\text{Fe}^{\text{IV}}\text{O}^{2+}$. However, the COD abatement was barely upgraded when the current density further increased to 28 mA cm^{-2} , attaining a final COD removal of 53.4%. Although the increase in current density gave rise to more efficient active chlorine accumulation, as depicted in Fig. 1, the destruction of refractory organics by active chlorine was fairly limited as mentioned previously, and excessive HClO can act as a scavenger of $\bullet\text{OH}$ via reaction (18) (Ye et al. 2016). Furthermore, high current density also caused greater extent of parasitic reactions (19) and (20), competing with the electrolysis of water to form $\text{M}(\bullet\text{OH})$ at the anode and the reduction of Fe^{3+} to regenerate Fe^{2+} at the cathode, respectively (Sirés et al. 2014).



On the contrary, more rapid $\text{NH}_4^+\text{-N}$ oxidation was observed at higher current density due to the

enhanced generation of active chlorine, which proved again that $\text{NH}_4^+\text{-N}$ elimination dominantly arose from the active chlorine oxidation, but barely affected by $\text{M}(\bullet\text{OH})$, $\bullet\text{OH}$ and $\text{Fe}^{\text{IV}}\text{O}^{2+}$ species.

Proposed reaction mechanism

Based on the results summarized in this work, the abatement mechanism of COD and $\text{NH}_4^+\text{-N}$ during the electrochemical assisted $\text{HClO}/\text{Fe}^{2+}$ treatment of old landfill leachate was proposed in Fig. 7. The active anode allowed effective electro-generation of active chlorine from the oxidation of chloride ions and the formation of a small amount of adsorbed $\text{M}(\bullet\text{OH})$, while the cathode supported the continuous reduction of Fe^{3+} to regenerate Fe^{2+} . The key reactions occurred between HClO and Fe^{2+} gave rise to highly active $\bullet\text{OH}$ and $\text{Fe}^{\text{IV}}\text{O}^{2+}$ in the bulk solution, and the generated chloride ions can be circularly oxidized at the anode. Therefore, COD in the leachate was mainly destructed by $\bullet\text{OH}$ and $\text{Fe}^{\text{IV}}\text{O}^{2+}$, in concomitance with partial oxidation by HClO and $\text{M}(\bullet\text{OH})$. On the other hand, active chlorine should be responsible for the $\text{NH}_4^+\text{-N}$ oxidation during the electrochemical treatment of landfill leachate.

Conclusion

The electrochemical assisted $\text{HClO}/\text{Fe}^{2+}$ process has been demonstrated as an effective technology for the treatment of old landfill leachate. The active anode, $\text{Ti}/\text{IrO}_2\text{-RuO}_2\text{-TiO}_2$, showed superior ability to generate active chlorine, which was more rapid in the presence of a greater Cl^- concentration or at a higher current density. The production of both $\bullet\text{OH}$ and $\text{Fe}^{\text{IV}}\text{O}^{2+}$ species was verified in the $\text{HClO}/\text{Fe}^{2+}$ system by employing DMSO and PMSO as the probes, respectively, despite the lower oxidizing potential of $\text{Fe}^{\text{IV}}\text{O}^{2+}$ compared with $\bullet\text{OH}$, it is

advantageous due to the high selectivity and activity for the oxidation of pollutants. The addition of Fe^{2+} to construct electrochemical assisted $\text{HClO}/\text{Fe}^{2+}$ system led to more rapidly abatement of COD, especially at the initial stage, than that in EO- HClO process. Acidic pH was found to favor better COD and NH_4^+ -N removal due to the fact that hypochlorous acid was the dominant active chlorine species at pH 3.0-8.0. The decay of COD was enhanced with the increase in Fe^{2+} dosage and current density to some extent, excessive high Fe^{2+} concentration and current density adversely caused many parasitic reactions, retarding either the accumulation of $\cdot\text{OH}$ and $\text{Fe}^{\text{IV}}\text{O}^{2+}$ in bulk or the reduction of Fe^{3+} at the cathode. Meanwhile, Fe^{2+} dosage showed negligible effect on NH_4^+ -N oxidation, which, nevertheless, could be largely promoted by increasing the applied current density. It was believed that various active species, including $\cdot\text{OH}$, $\text{Fe}^{\text{IV}}\text{O}^{2+}$, active chlorine and $\text{M}(\cdot\text{OH})$, could contribute to the COD abatement, and NH_4^+ -N removal highly relied on the oxidation by active chlorine during the electrochemical assisted $\text{HClO}/\text{Fe}^{2+}$ treatment of landfill leachate. In conclusion, this new approach is environmentally friendly and very promising for the treatment of wastewater containing high chloride content.

Data availability

All data and materials used during this study are included in the submitted manuscript and the supplementary files.

References

Abunama T, Othman F, Younes MK (2018) Predicting sanitary landfill leachate generation in humid regions using ANFIS modeling. *Environ Monit Assess* 190: 597.

364 Aguilar ZG, Brillas E, Salazar M, Nava JL, Sirés I (2017) Evidence of Fenton-like reaction with
 365 active chlorine during the electrocatalytic oxidation of acid yellow 36 azo dye with Ir-Sn-
 366 Sb oxide anode in the presence of iron ion. *Appl Catal B Environ* 206: 44-52.

367 Bunce NJ, Bejan D (2011) Mechanism of electrochemical oxidation of ammonia. *Electrochim*
 368 *Acta* 56 (24): 8085-8093.

369 Cabeza A, Urtiaga A, Rivero MJ, Ortiz I (2007) Ammonium removal from landfill leachate by
 370 anodic oxidation. *J Hazard Mater* 144: 715-719.

371 Costa AM, Alfaia RG de SM, Campos JC (2019) Landfill leachate treatment in Brazil – An
 372 overview. *J Environ Manag* 232: 110-116.

373 Deng Y, Chen N, Hu W, Wang H, Kuang P, Chen F, Feng C (2021) Treatment of old landfill
 374 leachate by persulfate enhanced electro-coagulation system: improving organic matters
 375 removal and precipitates settling performance. *Chem Eng J* 424: 130262.

376 Deng Y, Zhu X, Chen N, Feng C, Wang H, Kuang P, Hu W (2020) Review on electrochemical
 377 system for landfill leachate treatment: performance, mechanism, application, shortcoming,
 378 and improvement scheme. *Sci Total Environ* 745: 140768.

379 El Kateb M, Trellu C, Darwich A, Rivallin M, Bechelany M, Nagarajan S, Lacour S, Bellakhal
 380 N, Lesage G, Hérán M, Cretin M (2019) Electrochemical advanced oxidation processes
 381 using novel electrode materials for mineralization and biodegradability enhancement of
 382 nanofiltration concentrate of landfill leachates. *Water Res* 162: 446-455.

383 Fang JH, Cai Y, Shen S, Gu L (2022) New insights into FeS/persulfate system for tetracycline
 384 elimination: Iron valence, homogeneous-heterogeneous reactions and degradation
 385 pathways. *J Environ Sci* 112: 48-58.

386 Feng M, Cizmas L, Wang Z, Sharma VK (2017) Activation of ferrate (VI) by ammonia in
 387 oxidation of flumequine: kinetics, transformation products, and antibacterial activity
 388 assessment. *Chem Eng J* 323: 584-591.

389 Fernandes A, Pacheco MJ, Ciríaco L, Lopes A (2015) Review on the electrochemical processes
 390 for the treatment of sanitary landfill leachates: Present and future. *Appl Catal B: Environ*
 391 176-177: 183-200.

392 Fu S, Jia H, Meng X, Guo Z, Wang J (2021) Fe-C micro-electrolysis electrocoagulation based
 393 on BFDA in the pre-treatment of landfill leachate: enhanced mechanism and electrode
 394 decay monitoring. *Sci Total Environ* 781: 146797.

395 Gao Y, Zhou Y, Pang S, Wang Z, Shen Y, Jiang J (2020) Quantitative evaluation of relative
 396 contribution of high-valent iron species and sulfate radical in Fe(VI) enhanced oxidation
 397 processes via sulfur reducing agents activation. *Chem Eng J* 387: 124077.

398 Garcia-Espinoza JD, Mijaylova-Nacheva P, Aviles-Flores M (2018) Electrochemical
 399 carbamazepine degradation: effect of the generated active chlorine, transformation
 400 pathways and toxicity. *Chemosphere* 192: 142-151.

401 Ghahrchi M, Rezaee A (2021) Electrocatalytic ozonation process supplemented by EDTA-Fe
 402 complex for improving the mature landfill leachate treatment. *Chemosphere* 263: 127858.

403 Keyikoglu R, Karatas O, Rezaia H, Kobya M, Vatanpour V, Khataee A (2021) A review on
 404 treatment of membrane concentrates generated from landfill leachate treatment processes.
 405 Sep Purif Technol 259: 118182.

406 Kishimoto N, Nakamura Y, Kato M, Otsu H (2015) Effect of oxidation–reduction potential on
 407 an electrochemical Fenton-type process. Chem Eng J 260: 590-595.

408 Kwarciak-Kozłowska A, Fijałkowski KL (2021) Efficiency assessment of municipal landfill
 409 leachate treatment during advanced oxidation process (AOP) with biochar adsorption (BC).
 410 J Environ Manag 287: 112309.

411 Lai L, Zhou H, Zhang H, Ao Z, Pan Z, Chen Q, Xiong Z, Yao G, Lai B (2020) Activation of
 412 peroxydisulfate by natural titanomagnetite for atrazine removal via free radicals and high-
 413 valent iron-oxo species. Chem Eng J 387: 124165.

414 Liang S, Zhu L, Hua J, Duan W, Yang PT, Wang SL, Wei C, Liu C, Feng C (2020) $\text{Fe}^{2+}/\text{HClO}$
 415 reaction produces $\text{Fe}^{\text{IV}}\text{O}^{2+}$: an enhanced advanced oxidation process. Environ Sci Technol
 416 54: 6406-6414.

417 Mandal P, Yadav MK, Gupta AK, Dubey BK (2020) Chlorine mediated indirect electro-
 418 oxidation of ammonia using non-active PbO_2 anode: influencing parameters and
 419 mechanism identification. Sep Purif Technol 247: 116910.

420 Moreira FC, Boaventura RAR, Brillas E, Vilar VJP (2017) Electrochemical advanced oxidation
 421 processes: a review on their application to synthetic and real wastewaters. Appl Catal B
 422 Environ 202: 217-261.

423 Murrieta MF, Brillas E, Nava JL, Sires I (2020) Photo-assisted electrochemical production of
 424 HClO and Fe^{2+} as Fenton-like reagents in chloride media for sulfamethoxazole
 425 degradation. *Sep Purif Technol* 250: 117236.

426 Panizza M, Delucchi M, Sirés I (2010) Electrochemical process for the treatment of landfill
 427 leachate. *J Appl Electrochem* 40 (10): 1721-1727.

428 Reshadi MAM, Bazargan A, McKay G (2020) A review of the application of adsorbents for
 429 landfill leachate treatment: focus on magnetic adsorption. *Sci Total Environ* 731: 138863.

430 Shah AD, Liu Z, Salhi E, Höfer T, Gunten U (2015) Peracetic acid oxidation of saline waters in
 431 the absence and presence of H_2O_2 : secondary oxidant and disinfection byproduct
 432 formation. *Environ Sci Technol* 49: 1698-1705.

433 Shao B, Dong H, Sun B, Guan X (2018) Role of ferrate (IV) and ferrate (V) in activating ferrate
 434 (VI) by calcium sulfite for enhanced oxidation of organic contaminants. *Environ Sci*
 435 *Technol* 53: 894-902.

436 Silva AC, Dezotti M, Sant'Anna JrGL (2004) Treatment and detoxification of a sanitary landfill
 437 leachate. *Chemosphere* 55 (2): 207-214.

438 Sirés I, Brillas E (2012) Remediation of water pollution caused by pharmaceutical residues based
 439 on electrochemical separation and degradation technologies: a review. *Environ Int* 40: 212-
 440 229.

441 Sirés I, Brillas E, Oturan MA, Rodrigo MA, Panizza M (2014) Electrochemical advanced
 442 oxidation processes: today and tomorrow. A review. *Environ Sci Pollut Res* 21: 8336-8367.

443 Tai C, Peng JF, Liu JF, Jiang GB, Zou H (2004) Determination of hydroxyl radicals in advanced
 444 oxidation processes with dimethyl sulfoxide trapping and liquid chromatography. *Anal*
 445 *Chim Acta* 527: 73-80.

446 Vanlangendonck Y, Corbisier D, Van Lierde A (2005) Influence of operating conditions on the
 447 electro-oxidation rate in wastewaters from power plants (ELONITA™ technique). *Water*
 448 *Res* 39: 3028-3034.

449 Wang Z, Jiang J, Pang S, Zhou Y, Guan C, Gao Y, Li J, Yang Y, Qiu W, Jiang C (2018) Is sulfate
 450 radical really generated from peroxydisulfate activated by Iron(II) for environmental
 451 decontamination? *Environ Sci Technol* 52: 11276-11284.

452 Wu C, Liu J, Liu S, Li W, Yan L, Shu M, Zhao P, Zhou P, Cao W (2018) Assessment of the
 453 health risks and odor concentration of volatile compounds from a municipal solid waste
 454 landfill in China. *Chemosphere* 202: 1-8.

455 Yang Y, Liu Z, Demeestere K, Van Hulle S (2021) Ozonation in view of micropollutant removal
 456 from biologically treated landfill leachate: Removal efficiency •OH exposure, and
 457 surrogate-based monitoring. *Chem Eng J* 410: 128413.

458 Ye Z, Brillas E, Centellas F, Cabot PL, Sirés I (2020) Expanding the application of photoelectro-
 459 Fenton treatment to urban wastewater using the Fe(III)-EDDS complex. *Water Res* 169:
 460 115219.

461 Ye Z, Zhang H, Zhang X, Zhou D (2016) Treatment of landfill leachate using electrochemically
 462 assisted UV/chlorine process: effect of operating conditions, molecular weight distribution
 463 and fluorescence EEM-PARAFAC analysis. *Chem Eng J* 286: 508-516.

464 Zhang C, He D, Ma J, Waite TD (2018) Active chlorine mediated ammonia oxidation revisited:
465 reaction mechanism, kinetic modelling and implications. *Water Res* 145: 220-230.

466 Zhang J, Yang P, Zheng J, Li J, Jin S, Lv T, Zou YN, Xu P, Cheng C, Zhang Y (2020)
467 Degradation of gaseous HCHO in a rotating photocatalytic fuel cell system with an
468 absorption efficiency of up to 94%. *Chem Eng J* 392: 123634.

469 Zong Y, Shao Y, Zeng Y, Shao B, Xu L, Zhao Z, Liu W, Wu D (2021) Enhanced oxidation of
470 organic contaminants by iron(II)-Activated periodate: the significance of high-valent iron–
471 oxo species. *Environ Sci Technol* 55: 7634-7642.

472 Funding

473 This research was funded by the Fundamental Research Funds for the Central Universities, China
474 (No. 02190052020062) and the National Natural Science Foundation of China (No. 52100073).

475 Author information

476 Affiliations

477 **Department of Environmental Science and Engineering, School of Resource and**
478 **Environmental Sciences, Wuhan University, Wuhan 430079, China**

479 Zhihong Ye, Fei Miao and Hui Zhang

480 **Key Laboratory of Eco-environments in Three Gorges Reservoir Region, Ministry of**
481 **Education, College of Environment and Ecology, Chongqing University, Chongqing, China**

482 Zhihong Ye

483 Contributions

484 Zhihong Ye: Conceptualization, Methodology, Data collection, Formal analysis, Writing-
485 original draft, Funding acquisition.

486 Fei Miao: Methodology, Data collection, Formal analysis, Writing-review and edition.

487 Hui Zhang: Conceptualization, Methodology, Validation, Resources, Writing-review and edition,
488 Supervision.

489 Corresponding author

490 Correspondence to Hui Zhang.

491 Ethics declarations

492 Ethics approval

493 This study follows all ethical practices during writing.

494 Consent to participate

495 Not applicable

496 Consent for publication

497 Not applicable

498 Competing interests

499 The authors declare no competing interests.

Figures

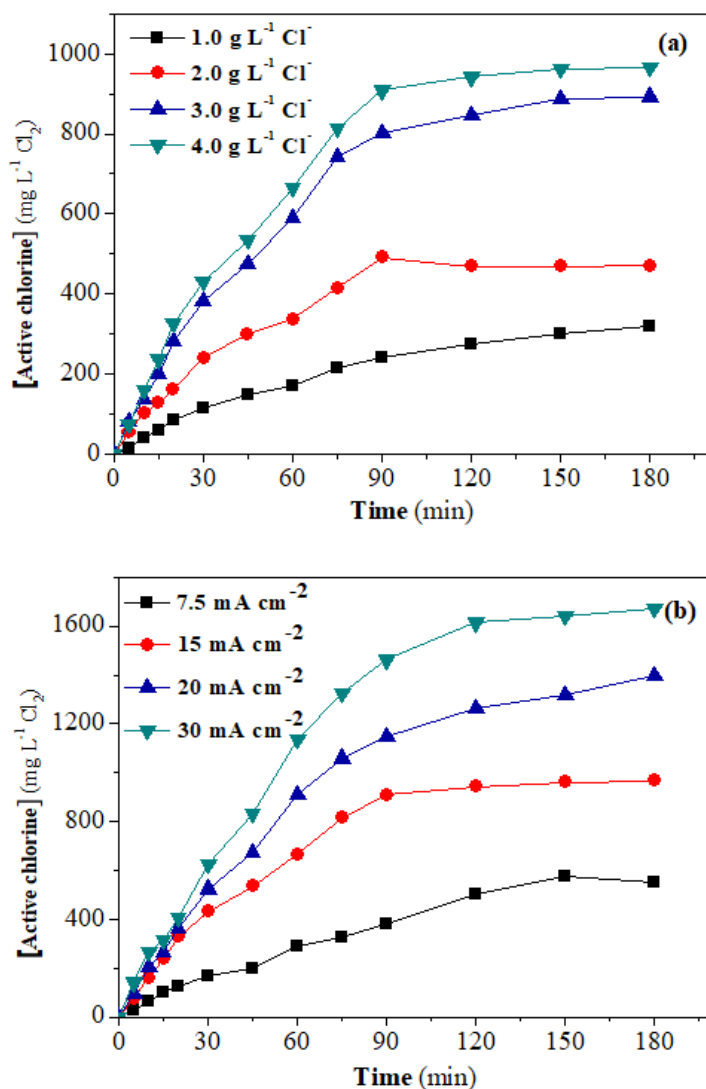


Fig. 1. Variation of active chlorine concentrations during the electrolysis of 400 mL solutions at pH 3.0 using a Ti/IrO₂-RuO₂-TiO₂ plate anode (25 cm²) and a titanium plate cathode. (a) Influence of initial Cl⁻ concentrations at current density of 15 mA cm⁻², Cl⁻ concentration: (■) 1.0 g L⁻¹, (●) 2.0 g L⁻¹, (▲) 3.0 g L⁻¹ and (▼) 4.0 g L⁻¹, (b) Influence of current density at an initial Cl⁻ concentration of 4 g L⁻¹, current density: (■) 7.5 mA cm⁻², (●) 15 mA cm⁻², (▲) 20 mA cm⁻² and (▼) 30 mA cm⁻².

Figure 1

See image above for figure legend

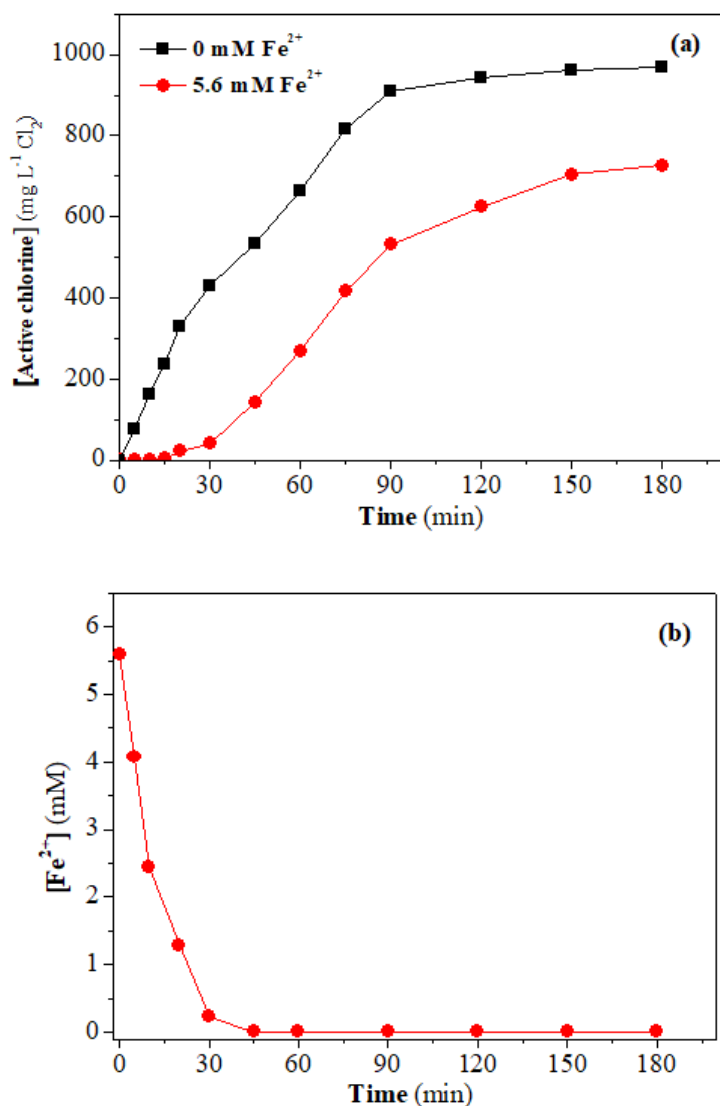


Fig. 2. (a) Time course of active chlorine concentration during the (■) EO (without Fe^{2+}) and (●) electrochemical assisted $\text{HClO}/\text{Fe}^{2+}$ (5.6 mM Fe^{2+}) processes at current density of 15 mA cm^{-2} , pH 3.0 and initial Cl^- concentration of 4.0 g L^{-1} using the same reactor described in Fig. 1; (b) Variation of Fe^{2+} concentration during electrochemical assisted $\text{HClO}/\text{Fe}^{2+}$ process in Fig. 2. (a).

Figure 2

See image above for figure legend

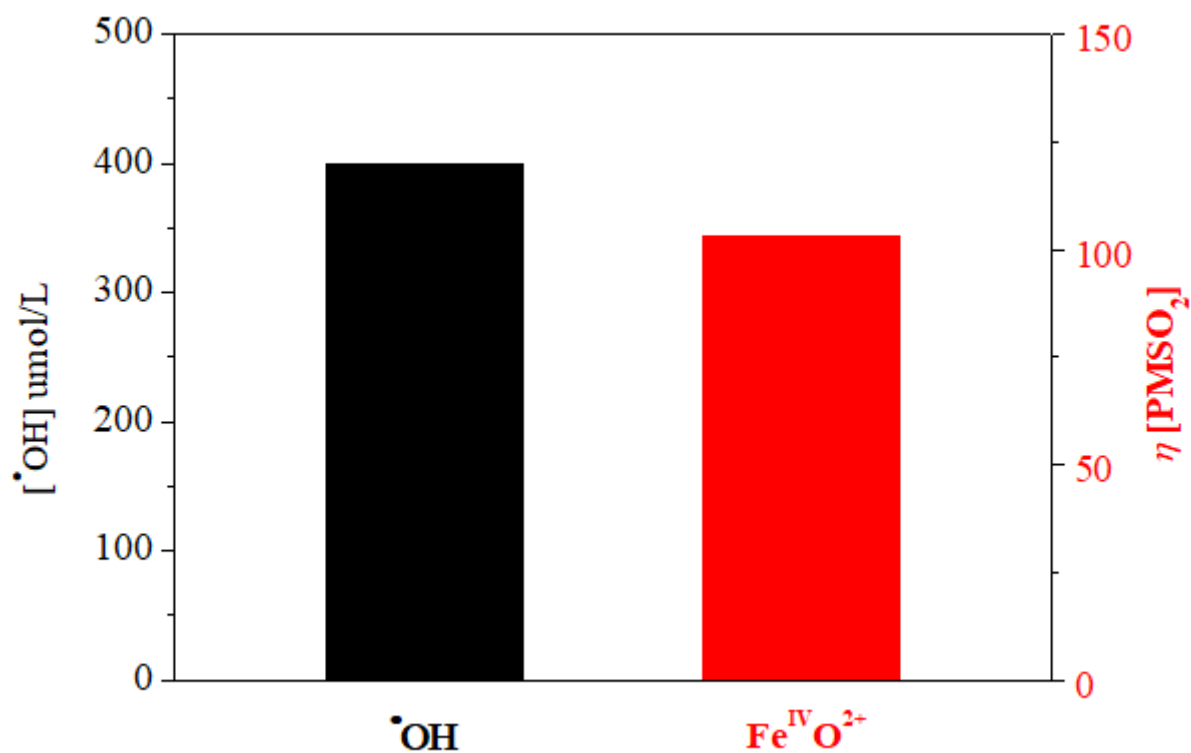


Figure 3

(a) Determination of apparent $\cdot\text{OH}$ amount (black) and FeIVO_2^+ yield (red) at pH 3.0 using DMSO ($\cdot\text{OH}$ probe) and PMSO (FeIVO_2^+ probe), respectively, in $\text{HClO}/\text{Fe}^{2+}$ system. $[\text{DMSO}] = 250 \text{ mM}$, $[\text{PMSO}] = 1.0 \text{ mM}$, $[\text{HClO}] = 8.0 \text{ mM}$ and $[\text{Fe}^{2+}] = 0.8 \text{ mM}$.

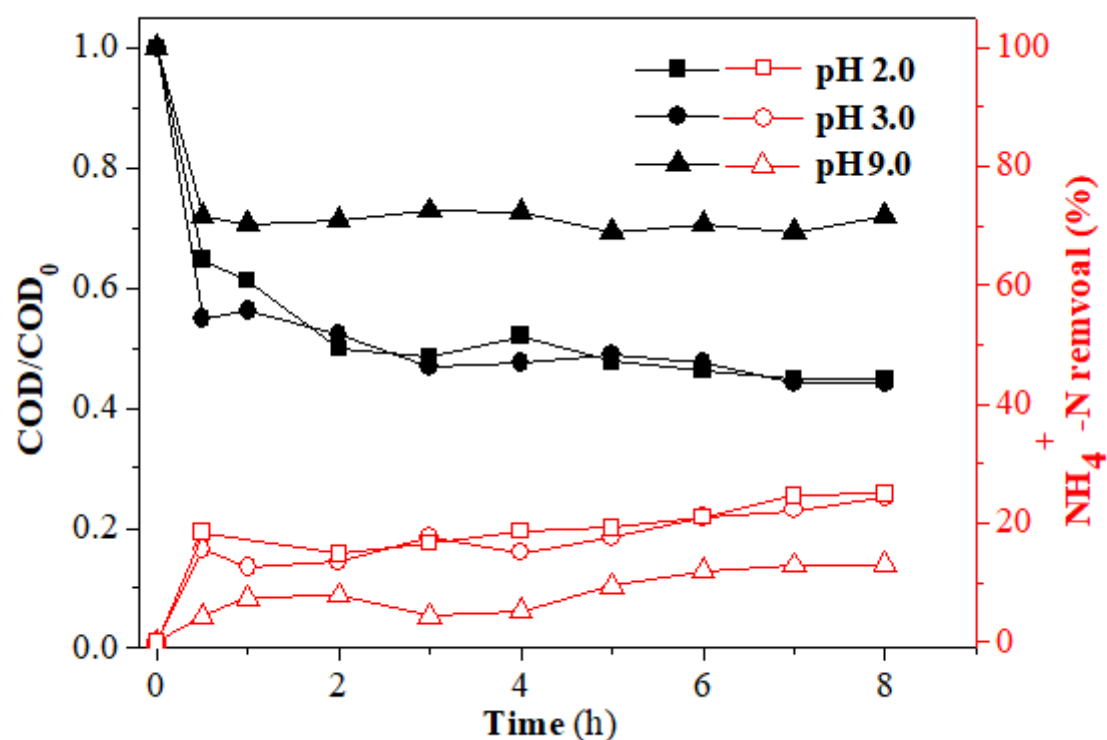


Figure 4

Effect of initial pH on the removal of COD and $\text{NH}_4^+\text{-N}$ with electrolysis time for the electrochemical assisted $\text{HClO}/\text{Fe}^{2+}$ treatment of 1 L landfill leachate with 4.0 mM Fe^{2+} at current density of 14 mA cm⁻² (black and solid: COD; red and hollow: $\text{NH}_4^+\text{-N}$).

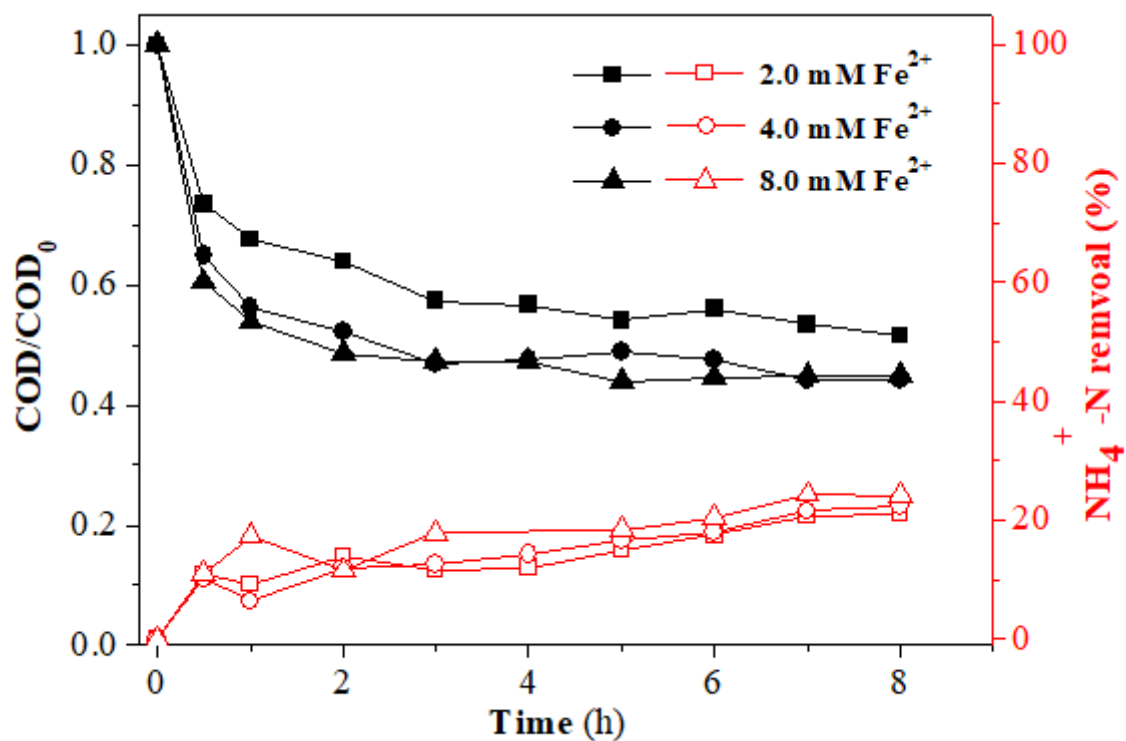


Figure 5

Influence of Fe^{2+} concentration on the time course of COD and $\text{NH}_4^+\text{-N}$ removal during the electrochemical assisted $\text{HClO}/\text{Fe}^{2+}$ treatment of 1 L landfill leachate at initial pH 3.0 and current density 14 mA cm^{-2} (black and solid: COD; red and hollow: $\text{NH}_4^+\text{-N}$).

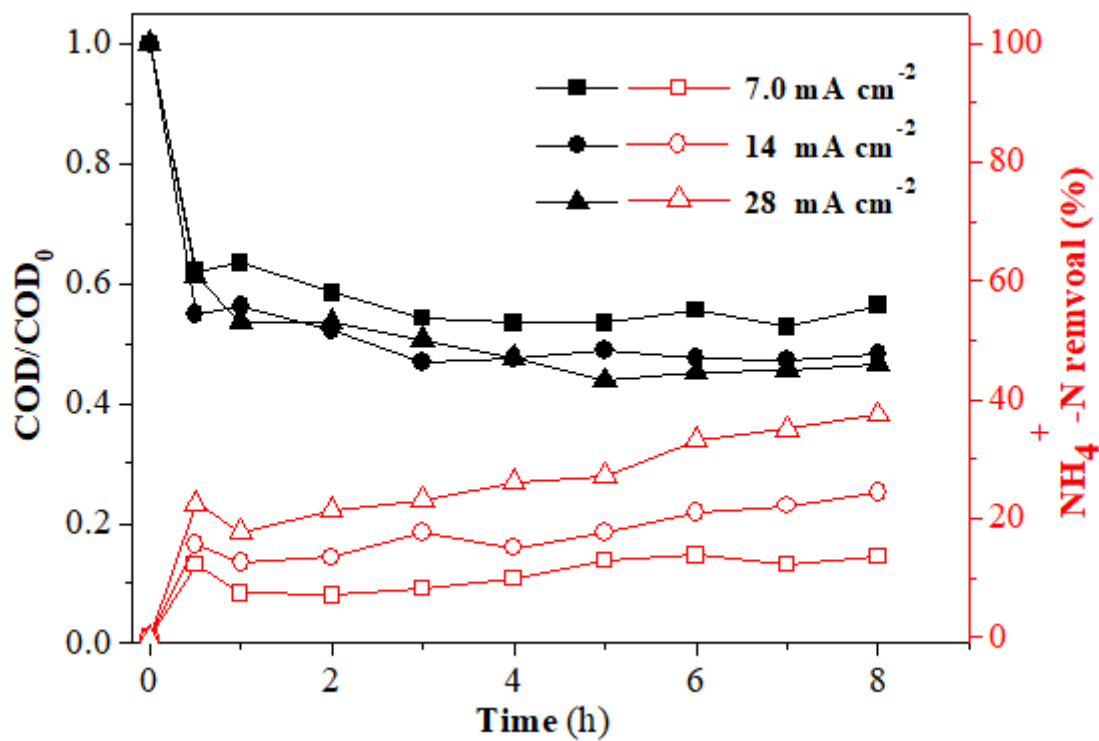


Figure 6

Effect of current density on the removal of COD and $\text{NH}_4^+\text{-N}$ during the electrochemical assisted $\text{HClO}/\text{Fe}^{2+}$ treatment of 1 L landfill leachate with 4.0 mM Fe^{2+} at initial pH 3.0 (black and solid: COD; red and hollow: $\text{NH}_4^+\text{-N}$).

